Transgenic Res (2011) 20:675–698
DOI 10.1007/s11248-010-9441-2

ORIGINAL PAPER

Gene expression profiling in the submandibular gland, stomach, and duodenum of CAVI-deficient mice

Pei-wen Pan · Katri Käyrä · Jukka Leinonen · Marja Nissinen · Seppo Parkkila · Hannu Rajaniemi

Received: 20 March 2010 / Accepted: 1 September 2010 / Published online: 11 September 2010

Abstract Carbonic anhydrase VI (CAVI) is the only secreted isozyme of the α-carbonic anhydrase family, which catalyzes the reversible reaction $CO_2 + H_2O \Leftrightarrow HCO_3^- + H^+$. It appears that CAVI protects teeth and gastrointestinal mucosa by neutralizing excess acidity. However, the evidence for this physiological function is limited, and CAVI may have additional functions that have yet to be discovered. To explore the functions of CAVI more fully, we generated *Car6*$^{-/-}$ mice and analyzed *Car6*$^{-/-}$ mutant phenotypes. We also examined transcriptomic responses to CAVI deficiency in the submandibular gland, stomach, and duodenum of *Car6*$^{-/-}$ mice. *Car6*$^{-/-}$ mice were viable and fertile and had a normal life span. Histological analyses indicated a greater number of lymphoid follicles in the small intestinal Peyer's patches. A total of 94, 56, and 127 genes were up- or down-regulated in the submandibular gland, stomach, and duodenum of *Car6*$^{-/-}$ mice, respectively. The functional clustering of differentially expressed genes revealed a number of altered biological processes. In the duodenum, the significantly affected biological pathways included the immune system process and retinol metabolic processes. The response to oxidative stress and brown fat cell differentiation changed remarkably in the submandibular gland. Notably, the submandibular gland, stomach, and duodenum shared one important transcriptional susceptibility pathway: catabolic process. Real-time PCR confirmed an altered expression in 14 of the 16 selected genes. The generation and of *Car6*$^{-/-}$ mice and examination of the effects of CAVI deficiency on gene transcription have revealed several affected clusters of biological processes, which implicate CAVI in catabolic processes and the immune system response.

Keywords Carbonic anhydrase · Gene knockout · Gene expression profiling · cDNA microarray

Abbreviations

ATP	Adenosine triphosphate
CA	Carbonic anhydrase

The authors Pei-wen Pan and Katri Käyrä contributed equally to this work.

P. Pan (✉) · S. Parkkila
Institute of Medical Technology, University of Tampere, Biokatu 6, 33520 Tampere, Finland
e-mail: peiwen.pan@uta.fi

S. Parkkila
School of Medicine, University of Tampere, Tampere, Finland

P. Pan · S. Parkkila
Centre for Laboratory Medicine, Tampere University Hospital, University of Tampere, Tampere, Finland

K. Käyrä · J. Leinonen · M. Nissinen · H. Rajaniemi
Department of Anatomy and Cell Biology, Institute of Biomedicine, University of Oulu, Oulu, Finland

ERG	Electroretinogram
ES	Embryo stem
GO	Gene ontology
PAGE	Polyacrylamide gel electrophoresis
PBS	Phosphate-buffered saline
qRT–PCR	Quantitative real-time polymerase chain reaction
RT-PCR	Reverse transcription-polymerase chain reaction
SDS	Sodium dodecyl sulfate
TK	Thymidine kinase
VLAD	Visual annotation display

Introduction

The α-carbonic anhydrases (α-CAs) form a large family of zinc-containing enzymes expressed in most mammalian organs. They participate in a variety of physiological processes including pH regulation, CO_2 and ion transport, and water and electrolyte balance. They catalyze the reversible reaction: $CO_2 + H_2O \Leftrightarrow HCO_3^- + H^+$ (Sly and Hu 1995). To date, 16 isoforms have been characterized, 13 of which have been found to be enzymatically active (Hilvo et al. 2005; Kivela et al. 2005; Lehtonen et al. 2004; Pastorekova et al. 2004). Since several isozymes are expressed in the same cells and tissues, they may be mutually complementary to each other in physiological processes, and their regulation may be at least partly interconnected (Pan et al. 2006).

Carbonic anhydrase isozyme VI (CAVI) is the only secreted isozyme in this enzyme family (Fernley et al. 1979; Murakami and Sly 1987). It is secreted into saliva by serous acinar cells of the parotid, submandibular (Parkkila et al. 1990), and lingual von Ebner's glands (Amasaki et al. 2003; Leinonen et al. 2001) and into milk by the mammary glands (Karhumaa et al. 2001). Recently this enzyme has been found in the lacrimal glands (Ogawa et al. 2002), nasal, septal, and lateral glands (Kimoto et al. 2004), esophagus (Kasuya et al. 2007; Murakami et al. 2003), tracheobronchial glands, epithelial serous cells (Leinonen et al. 2004), and alimentary canal (Kaseda et al. 2006). Low concentrations of CAVI have also been detected in serum (Kivela et al. 1997). Moreover, evidence has been obtained by RT-PCR for CAVI mRNA expression in the stomach, intestine, gallbladder, liver, and pancreas (Fujikawa-Adachi et al. 1999). An intracellular, non-secreted, stress-inducible form of CAVI has also been described in mouse fibroblasts (Sok et al. 1999).

Although CAVI has been studied for 30 years, its exact physiological role has remained unclear. Recent studies have suggested that salivary CAVI may protect teeth from caries (Kimoto et al. 2006) and the esophageal and gastric epithelium from acid injury (Parkkila et al. 1997). An interesting growth-promoting role of CAVI in taste buds has also been suggested by Henkin et al. (Henkin et al. 1999). In addition, CAVI may be an essential maturation-promoting factor in the alimentary tract because high amounts of CAVI are delivered to infants' alimentary tract in colostral milk (Karhumaa et al. 2001).

At present, various CA inhibitors and gene-targeted animal models are the approaches most commonly used to elucidate the physiological function of CA isozymes. In addition to the CAII-deficient mice produced by chemical mutagenesis (Lewis et al. 1988), knockout mice for the isozymes III, IV, IX, and XIV have been generated by targeted mutagenesis (Gut et al. 2002; Kim et al. 2004; Leppilampi et al. 2005; Shah et al. 2005). Surprisingly, the latter mice have shown only mild phenotypic changes. Mice deficient in CAXIV show a significant reduction in retinal light response as measured by electroretinogram (ERG) (Ogilvie et al. 2007). This functional defect is more severe in the doubly deficient CAIV/CAXIV knockout mice. CAIX deficiency produces a clear gastric phenotype with hyperplasia of the mucosal epithelium (Gut et al. 2002). Similarly, some of the CAII-deficient mice have been found to exhibit mild gastric hyperplasia. CAII-deficient mice also lack the duodenal bicarbonate secretory response to prostaglandin E_2 (Leppilampi et al. 2005). According to the first report (Kim et al. 2004), CAIII-deficient mice showed no abnormal phenotype, but more recently, CAIII deficiency has been linked to impaired mitochondrial ATP synthesis in mice subjected to high-intensity exercise (Liu et al. 2007).

Microarray-based gene expression profiling provides the opportunity to simultaneously measure the expression level of tens of thousands of mRNAs in a given transcriptome. It has been widely used to study the general transcriptional expression profiles as well as individual genes involved in disease processes (Morey et al. 2006). It also has the potential to

elucidate the global alteration in gene expression and altered biological processes induced by modern genetic tools such as targeted mutagenesis.

The present study describes the generation of *Car6*$^{-/-}$ mice, examination of *Car6*$^{-/-}$ phenotypes, and application of a cDNA microarray to analyze the transcriptomes of the submandibular gland, stomach, and duodenum of *Car6*$^{-/-}$ and wild-type mice.

Materials and methods

Isolation of the mouse *Car6* gene

A partial mouse *Car6* DNA sequence was amplified from genomic DNA extracted from the blood of three mice. Primers were designed according to the mouse *Car6* sequence deposited in GenBank (Accession NC_000070): P5a, 5′-GGAGAAAACCTACAACTC TGAA-3′; P5b, 5′-GTGACTCTGTCTCTAAGCAC-3′. The amplified mouse *Car6* DNA was confirmed by sequencing and then labeled with ^{32}P using the Rediprime II Random Prime Labeling System (Amersham). The labeled probe was used to screen a 129/Svj mouse strain lambda FIX® II library (Stratagene) in order to isolate the entire mouse *Car6* gene. Prehybridization, hybridization, and washes were performed according to standard procedures (Sambrook et al. 1989). Secondary and tertiary screenings were also carried out as outlined in standard methodology texts (Sambrook et al. 1989).

The resulting clone containing the entire mouse *Car6* gene was identified by partial sequencing and restriction mapping and then used as a template to construct the targeting vector.

Construction of *Car6* targeting vector

The targeting vector used for disruption of the *Car6* locus by homologous recombination is shown in Fig. 1A. The vector (pPN2ThGHterm-*Car6* targeting vector) was designed such that exons 2 and 3 of the mouse *Car6* gene were replaced by the bacterial neomycin resistance gene (Neo). This disrupted the domains of the CAVI molecule that are required for proper conformation (the cysteine residue at position 41) and enzyme activity (conserved histidines at positions 84, 110, and 112). The pPN2ThGHterm vector (Zhu et al. 1999), consisting of a neo-resistance cassette (neo), two herpes simplex virus thymidine kinase (TK) cassettes, and a pUC19 vector backbone was used to construct the *Car6* targeting vector.

To construct the pPN2ThGHterm-*Car6* targeting vector, a short 5′-homologous arm (2058 bp) containing exon 1 was amplified using the entire mouse *Car6* gene clone (described above) as a template. The primers used were P3a (5′-TATGACTGCGGCC GCCACTCTCTAATCCCATACTCAG-3′) and P3b (5′- TGACTCCTGCAGGCAATGGAGCTGAGGTA GAGTGT-3′), which include a *Not*I and an *Sse*8387I restriction site, respectively, in addition to several extra bases at the 5′-end of both strands. The product obtained was then inserted upstream of the Neo cassette in pPN2ThGHterm in order to produce the pPN2ThGHterm-*Car6* arm 1 vector. Subsequently, a long 3′-homologous arm (4984 bp) containing exons 4 and 5 was amplified using the entire mouse *Car6* gene clone as a template. The primers used in the amplification were HAF (5′-TTCATTGGATCCACC TATGAGAATGCCAAGGA-3′) and HAR2 (5′-TT CATTGAATTCTTGATTCATGTGCCTGGACT-3′), which contained a *Bam*HI and an *Eco*RI restriction site, respectively, in addition to several extra bases at the 5′-end of both strands. The product obtained was inserted between the Neo cassette and the TK cassettes of the pPN2ThGHterm-*Car6* arm 1 vector to generate the pPN2ThGHterm-*Car6* targeting vector. The final pPN2ThGHterm-*Car6* targeting vector was linearized by NotI digestion and introduced into mouse embryonic stem (ES) cells by electroporation.

Screening of mouse ES cell clones

To determine whether the *Car6* gene had been successfully disrupted, genomic DNA samples extracted from about 300 selected ES cell clones were subjected to multiplex PCR. Primers F1 (5′-AGG GAGGGGCTGTGCTCGAA-3′), R1 (5′-GGATCC AGCTTGTTAGGCTT-3′), and R2 (5′-GGCCTA CCCGCTTCCATTGC-3′) were designed so that the wild-type *Car6* locus produces a 2,322-bp fragment by PCR using primers F1 and R1, while the targeted locus produced a 2,561-bp fragment using primers F1 and R2 (Fig. 1A). A 5′-probe (2,006 bp) amplified using primers 5′-probeF (5′-TGGAGAGATGGCTCAGA AGT-3′) and 5′-probeR (5′-AACTCACAAGAGGT CTGGCT-3′) was utilized to confirm the disrupted

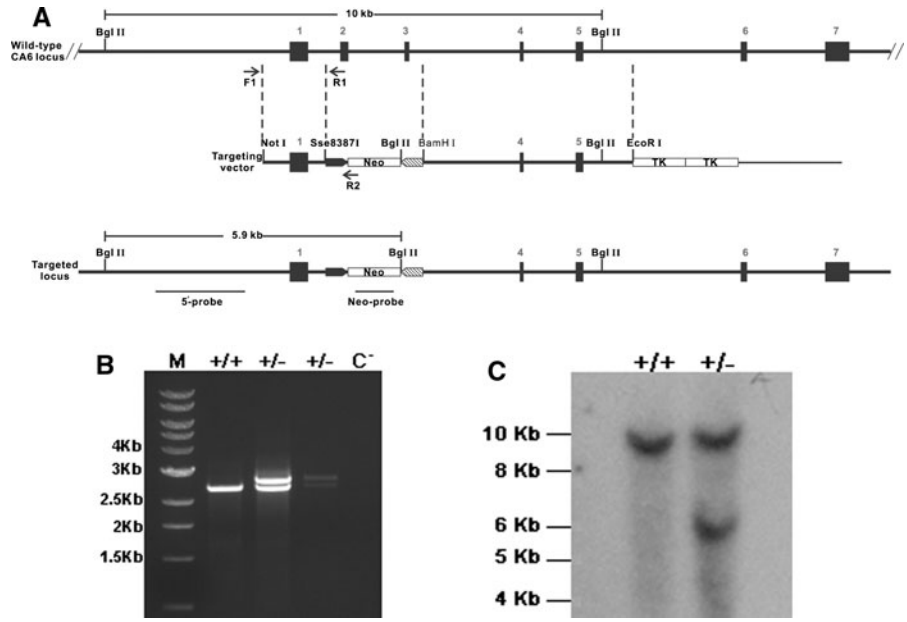

Fig. 1 Targeted disruption of the *Car6* gene in ES cells. **A** A schematic representation of the disruption of the *Car6* locus by homologous recombination. *Solid boxes* represent exons. F1, R1, and R2 are primers used for genotyping. **B** Identification of targeted (+/−) ES cell clones using multiplex PCR. *M* molecular marker. C^- indicates the negative control for PCR (H_2O). **C** Characterization of targeted (+/−) ES cell clones by Southern blot

Car6 locus by Southern blot. In addition, a Neo probe (743 bp) was amplified using primers NeoF (5′-GA GAGGCTATTCGGCTATGA-3′) plus NeoR (5′-GA AGAACTCGTCAAGAAGGC-3′) and applied in Southern blotting to verify that only one copy of the Neo cassette had been integrated correctly into the mouse genome.

Mouse breeding

Targeted ES cells were injected into C57BL/6 blastocysts and implanted into pseudopregnant mice. Chimeras were identified by coat color. Male chimeras were mated to C57BL/6 females to test germ-line transmission and to create offspring that were heterozygous for the *Car6* deletion. Genotyping of offspring was carried out by multiplex PCR on genomic DNA using primers F2 (5′-CCTGGAGTT-CACTATGACTAAC-3′), R1, and R2: a 434-bp product was obtained by F2 plus R1 for wild-type, while a 673-bp product was obtained by F2 plus R2 for $Car6^{-/-}$. The mice with the targeted allele were backcrossed with the C57BL/6 strain for 10 generations. Heterozygotes were intercrossed to produce mice that were homozygous for the targeted gene. $Car6^{-/-}$ knockout mice proved to be fertile, and the mice originating from knockout intercrossings were subjected to phenotypic analysis. The production of the knockout mouse line was approved by the Animal Experimentation Committee of the University of Oulu. The mice were housed in pathogen-free conditions. The health status of the animals was monitored on a regular basis in accordance to the FELASA recommendations. The sizes of litters were recorded for control mice crossing and $Car6^{-/-}$ mice crossing for the determination of fertility. Life span was determined by recoding the death of control and $Car6^{-/-}$ mice weekly.

Histological and immunohistochemical analysis

Tissue samples were taken from the following areas of wild-type and $Car6^{-/-}$ adult mice: submandibular gland, parotid gland, lacrimal gland, mammary gland, tongue, trachea, and nasal cavity. The samples were dissected, fixed in Carnoy's fluid or in 4% paraformaldehyde for 8–18 h, embedded in paraffin, and sectioned to a thickness of 5 μm. Sections were stained with hematoxylin and eosin. The immunohistochemical staining was performed using a polyclonal rabbit anti-rat CAVI serum (Leinonen et al. 2001) preabsorbed as described below. Prior to immunostaining, the sections were boiled in 10 mM sodium citrate buffer (pH 6) to improve the penetration of the reagents and, thereafter, treated with H_2O_2 in phosphate-buffered saline (PBS) for five min to

remove endogenous peroxidase. A Histostain-Plus broad-spectrum kit (Zymed Laboratories) was used following the manufacturer's guidelines.

To improve the specificity of the rat antiserum to CAVI, it was preabsorbed with the 56-kDa protein present in the mouse parotid gland. Proteins of the parotid gland extract obtained from a *Car6*$^{-/-}$ mouse were separated on a 10% SDS–polyacrylamide gel and transferred to a polyvinylidene fluoride (PVDF) membrane. The 56-kDa protein band on the PVDF membrane was cut out and incubated in 4% bovine serum albumin/phosphate-buffered saline with Tween-20 (BSA/PBST) for 1 h at room temperature. Subsequently, the anti-rat CAVI serum (diluted 1:300) was incubated overnight in 4% BSA/PBST/0.01% NaN_3 with the membrane strip containing the 56-kDa protein. The preabsorbed antiserum was used for immunohistochemical staining (diluted 1:200) and western blotting (diluted 1:10,000). Immunostaining was performed as previously described (Karhumaa et al. 2001). Sections were examined using the Nikon Eclipse E600 microscope and photographed with Micropublisher 5.0 RTV and Qimaging computer software (Qimaging, Canada).

Western blotting

Submandibular and parotid gland tissue samples from wild-type and *Car6*$^{-/-}$ mice were homogenized in 0.5 ml of buffer containing 0.1 M Tris–SO_4, 0.2 M sodium sulfate, and 1 mM benzamidine at pH 8.7. The homogenates were centrifuged for 30 min at 25,000×*g* at 4°C, and the protein content of the supernatants was determined using the Bio-Rad Protein Assay and an Eppendorf BioPhotometer. Aliquots of the supernatants (15 μg) were mixed with SDS sample buffer, and SDS–PAGE was performed as described by Laemmli (Laemmli 1970). Separated proteins were transferred to the PVDF membrane and immunostained using preabsorbed or non-preabsorbed anti-rat CAVI serum as described earlier (Karhumaa et al. 2001).

pH value measurement

Four wild-type and eight *Car6*$^{-/-}$ adult mice were subjected to the pH value measurement. The mice were provided only with water 1 day before the experiment and sacrificed by the cervical dislocation method. The stomach and duodenum were immediately exposed and isolated by sutures in the cardioesophageal junction, pylorus, and the end of duodenum. 300 and 500 μl sterile distilled water was injected into the duodenum and stomach, respectively, and the pH value of the obtained water sample was measured.

cDNA microarray analysis

Submandibular gland, stomach, and duodenum samples were collected from three wild-type and three *Car6*$^{-/-}$ female mice, respectively, of 2 months of age. Total RNAs were purified using the RNeasy Mini Kit (Qiagen, Basel, Switzerland). On-column DNase digestion was performed during the RNA purification process. RNA concentrations, A260/280, and A260/230 ratios were determined using a ND-1000 spectrophotometer (Nanodrop Technologies, Wilmington, USA). All above-mentioned 18 RNA samples were analyzed separately using Illumina's Sentrix® MouseRef-8 v2 BeadChip in the Finnish DNA Microarray Center at Turku Center for Biotechnology. RNA amplification and hybridization were performed as described before (Rodriguez et al. 2009). The obtained microarray data set has been deposited in the NCBI Gene Expression Omnibus (GEO, http://www.ncbi.nim.nih.gov/geo/) and is accessible through GEO Series accession number GSE 20423.

Data analyses

Microarray data were analyzed using Chipster v1.3.0 as described by Rodriguez et al. (Rodriguez et al. 2009). After the filtering of probes according to their standard deviation, the remaining 151 probes were subjected to statistical analysis using the empirical Bayes *t* test for the comparison of two groups. No filtering was applied to the data according to *P*-values at this step because of the small sample number. The statistical results were considered indicative of orientation and the 151 probes were ranked by fold change. The expression levels of genes were considered altered when a fold change greater than ±1.4 was observed. Functional annotation of differentially transcribed genes was performed using VLAD (http://proto.informatics.jax.org/prototypes/vlad/) according to the online instruction.

Quantitative real-time PCR (qRT-PCR) validation

Some of the results obtained from the cDNA microarray analyses were validated by qRT-PCR. Genes were selected for qRT-PCR based on their fold change and known function. In addition, the expression level of all 13 enzymatically active CAs was quantified. Gene descriptions, primer sequences, product sizes, and annealing temperatures for these genes and the house-keeping gene *GAPDH* are shown in Table 1. Total RNA from each of the above-mentioned six female mice (three wild types and three *Car6*$^{-/-}$ mice used in the cDNA microarray analyses) and six male mice (three wild types and three *Car6*$^{-/-}$ mice) was reverse transcribed using a High capacity cDNA reverse transcription kit (Applied Biosystems Inc, CA, USA) according to the manufacturer's instructions. Duplicate qRT-PCR reactions were performed with PowerSYBR SybrGreen reagents (Applied Biosystems Inc, CA, USA) on an ABI7000 Real Time PCR System (Applied Biosystems Inc, CA, USA). The final qRT-PCR results were presented as the relative expression of the gene-of-interest to the house-keeping gene *GAPDH*.

Statistical analyses

An unpaired Student *t* test was used to evaluate the significance of defferences in mRNA expression in wild-type and *Car6*$^{-/-}$ mice detected by qRT-PCR. The same test was performed for the evaluation of difference in lymphoid follicle levels in Peyer's patches.

Results

The generation and validation of *Car6* gene disruption

In order to investigate the function of CAVI, we generated *Car6*$^{-/-}$ knockout mice. The successful disruption of the *Car6* allele was demonstrated in two of 300 selected drug-resistant embryonic stem (ES) cell clones using PCR analysis and Southern blotting (Fig. 1B, C). After injection of these two ES cell clones into C57BL/6 blastocysts and subsequent implantation into pseudopregnant mice, 46 chimeras were identified by coat color. Three male chimeras from each clone were mated to C57BL/6 females and all six chimeras displayed germ-line transmission: the offspring from the intercrosses contained the three expected genotypes at Mendelian frequencies (Fig. 2A). The resulting *Car6*$^{+/-}$ heterozygotes and *Car6*$^{-/-}$ homozygotes were healthy and fertile, and had normal life spans. Similarly, the litter size and development of the pups did not deviate from the wild-type mice. The disappearance of the 37-kDa CAVI polypeptide in the western blots showed that the homozygous *Car6*$^{-/-}$ mice expressed no CAVI protein in their salivary glands (Fig. 2B), while the heterozygous *Car6*$^{+/-}$ mice expressed less CAVI protein as compared to wild-types. Western blotting of parotid gland extracts using non-preabsorbed anti-CAVI serum detected a larger immunoreactive protein of $\sim$ 56 kDa. A similar 56-kDa polypeptide was often detected in the CAVI protein fraction after affinity chromatography purification from human saliva. This band has been recently identified by mass spectrometry as salivary α-amylase (data not shown).

Elimination of CAVI in the knockout mice was further confirmed by immunohistochemical staining. Very faint signals, or none at all, were observed in the submandibular glands of *Car6*$^{-/-}$ mice using non-preabsorbed anti-CAVI serum (Fig. 3B) whereas substantial staining was detected in wild-type mice (Fig. 3A). The non-preabsorbed serum showed a positive reaction in the serous cells of the parotid glands of *Car6*$^{-/-}$ mice, but this reaction was absent when the antiserum was preabsorbed with the 56-kDa protein. This result suggests that the antiserum contains contaminating antibodies which react with the 56-kDa protein (Fig. 3C–F). It is worth noting that the rat submandibular gland shows significantly lower levels of α-amylase mRNA than the parotid gland (Nezu et al. 2002), which provides indirect confirmation that the 56-kDa protein is, indeed, salivary α-amylase. As observed in western blots, we found that in the submandibular gland the staining of CAVI was strongest in wild-type mice, while weaker staining was detected for *Car6*$^{+/-}$ mice (Fig. 4). This finding suggests the gene copy number of *Car6* has effect on the protein expression.

Histopathological and macroscopic analyses

Histopathological and macroscopic analyses of gastrointestinal samples collected from knockout and

Table 1 Genes evaluated by qRT-PCR

Gene	Primer sequences (5′-3′)	Amplicon size (bp)	Tm (°C)
Carbonic anhydrase 1 (Car1)	F: TTGATGACAGTAGCAACC	161	51
	R: CCAGTGAACTAAGTGAAG		
Carbonic anhydrase 2 (Car2)	F: CAAGCACAACGGACCAGA	122	56
	R: ATGAGCAGAGGCTGTAGG		
Carbonic anhydrase 3 (Car3)	F: GCTCTGCTAAGACCATCC	160	54
	R: ATTGGCGAAGTCGGTAGG		
Carbonic anhydrase 4 (Car4)	F: CTCCTTCTTGCTCTGCTG	145	55
	R: GACTGCTGATTCTCCTTA		
Carbonic anhydrase 5a (Car5a)	F: ACCAAAGCAAGGGCATACAG	104	58
	R: TGGCACAGAGAAGTCCCACA		
Carbonic anhydrase 5b (Car5b)	F: AATGGCTTGGCTGTGATAGG	187	60
	R: GGCGTAGTGAGAGACCCAGA		
Carbonic anhydrase 6 (Car6)	F: AAGATTGACGAGTATGCC	145	54
	R: TAGGTGTAATAGTGGTGG		
Carbonic anhydrase 7 (Car7)	F: CAATGACAGTGATGACAGAA	160	55
	R: TCCAGTGAACCAGATGTAG		
Carbonic anhydrase 9 (Car9)	F: CTGAAGACAGGATGGAGAAG	221	57
	R: GCAGAGTGCGGCAGAATG		
Carbonic anhydrase 12 (Car12)	F: CCTATGTTGGTCCTGCTG	143	53
	R: CGTTGTAACCTTGGAACTG		
Carbonic anhydrase 13 (Car13)	F: AATACGACTCCTCACTCC	116	52
	R: TGCCGCAACCTGTAGTTC		
Carbonic anhydrase 14 (Car14)	F: TGTTGTTCTTCGCTCTCCTG	161	53
	R: CACTGTCTGTCTGGATATTG		
Carbonic anhydrase 15 (Car15)	F: AGCACAGCCTGGATGAGA	170	55
	R: CAGACACAATGGCAGAGA		
Alcohol dehydrogenase 7 (class IV), mu or sigma polypeptide (Adh7)	F: TAGAAGAGTGAACCGTGCCT	111	60
	R: GGACAGCCGCTTTGCACTTA		
Asparagine-linked glycosylation 5 homolog (yeast, dolichyl-phosphate beta-glucosyltransferase) (Alg5)	F: CTATCTGTTGTTGTGCCTTC	135	58
	R: TGCCATCGTCAACCACTATC		
Advillin (Avil)	F: GGTCAGTTCCAGGAAGACAG	141	60
	R: CTCGTAGAAGTTGCCGTGAG		
BRF1 homolog, subunit of RNA polymerase III transcription initiation factor IIIB (S. cerevisiae) (Brf1)	F: AAGGAATCAAGAGCACAGAC	182	58
	R: AACCAAGTAGAGGCAGGCAG		
Claudin 18 (Cldn18)	F: GGCCATACTTCACCATCCTG	142	60
	R: CTACCAATGCGAATGCACTT		
Glyseraldehyde-3-phosphate dehydrogenase (GAPDH)	F: ATGGTGAAGGTCGGTGTG	186	56
	R: CATTCTCGGCCTTGACTG		
Gastrin (Gast)	F: GCCACAACAGCCAACTATTC	82	58
	R: TAGAGCCAGCACTAAGACCA		
Glucosaminyl (N-acetyl) transferase 1, core 2 (Gcnt1)	F: GATTCAGGCTTCCTGTGATT	145	58
	R: ATTCAGAGGCTTCCTGGTGT		

Table 1 continued

Gene	Primer sequences (5′-3′)	Amplicon size (bp)	Tm (°C)
Gastric intrinsic factor (Gif)	F: CAGTGACAGTGCAGACCTGA	124	58
	R: AAGGTGACCAGTTCTCCATT		
Gastrokine 1 (Gkn1)	F: ATCCTCTGCTCCACCACACT	143	60
	R: ACTGCTGTCCACTTCCGTCT		
ISG15 ubiquitin-like modifier (Isg15)	F: GACCTAGAGCTAGAGCCTG	89	60
	R: GGAGTTAGTCACGGACACCA		
Lymphocyte antigen 6 complex, locus G6E (Ly6g6e)	F: AGACTGCTGAGCTGTACCTG	173	60
	R: ACCTCGTCCTCTCGACACT		
2-5 Oligoadenylate synthetase-like 2 (Oasl12)	F: GGTGATTAAGGTGGTGAAGG	178	58
	R: CCAGGCTTCTGCTACAATGA		
Secreted phosphoprotein 1 (Spp1)	F: AGAATGCTGTGTCCTCTGAA	120	58
	R: TGGTCTCCATCGTCATCATC		
Ubiquitin specific peptidase 18 (Usp18)	F: TGAAGAGGAAGAGAGTGCTG	87	58
	R: GTCTGTCCGATGTTGTGTAA		

F forward primer, *R* reverse primer, *Tm* annealing temperature

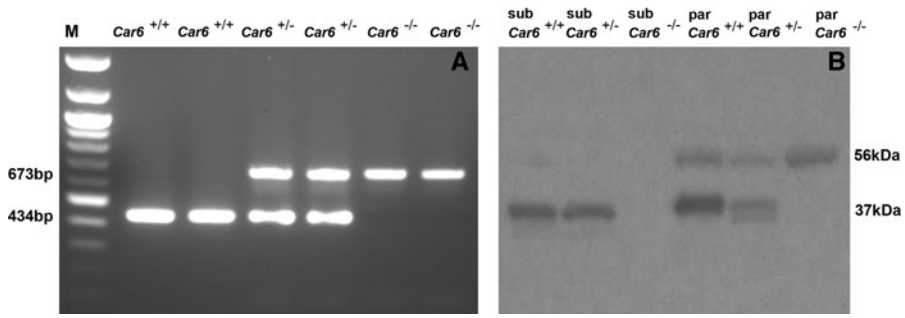

Fig. 2 Validation of *Car6*$^{-/-}$ mice. **A** Genotyping of wild-type, heterozygous *Car6*$^{+/-}$, and homozygous *Car6*$^{-/-}$ mice using PCR. *M* molecular marker. **B** Western blotting of protein extracts from the submandibular (sub) and parotid (par) glands of wild-type, *Car6*$^{+/-}$ and *Car6*$^{-/-}$ mice. Non-preabsorbed anti-CAVI antiserum was used

control mice at 2 months of age revealed that the number of lymphoid follicles in Peyer's patches was substantially higher in adult knockout mice than in control mice (Table 2). No other macroscopic or histological differences were observed between the knockout and control mice.

pH values in the stomach and duodenum

Table 3 shows the result of the pH value measurement in the stomach and duodenum of the wild-type and *Car6*$^{-/-}$ mice. No significant difference was observed between these two groups.

cDNA microarray analysis

In an effort to identify genes with altered transcription in tissues of *Car6*$^{-/-}$ mice, the transcriptomes of the submandibular gland, stomach, and duodenum from three wild-type mice and three *Car6* knockouts were analyzed and compared. Considering a threshold of at least a 1.4-fold change in expression, we observed 27 genes with increased expression and 67 genes with reduced expression in the submandibular gland of *Car6*$^{-/-}$ mice as compared to wild-type mice. The numbers of up- and down-regulated genes detected in the stomach of *Car6*$^{-/-}$ mice were 14 and

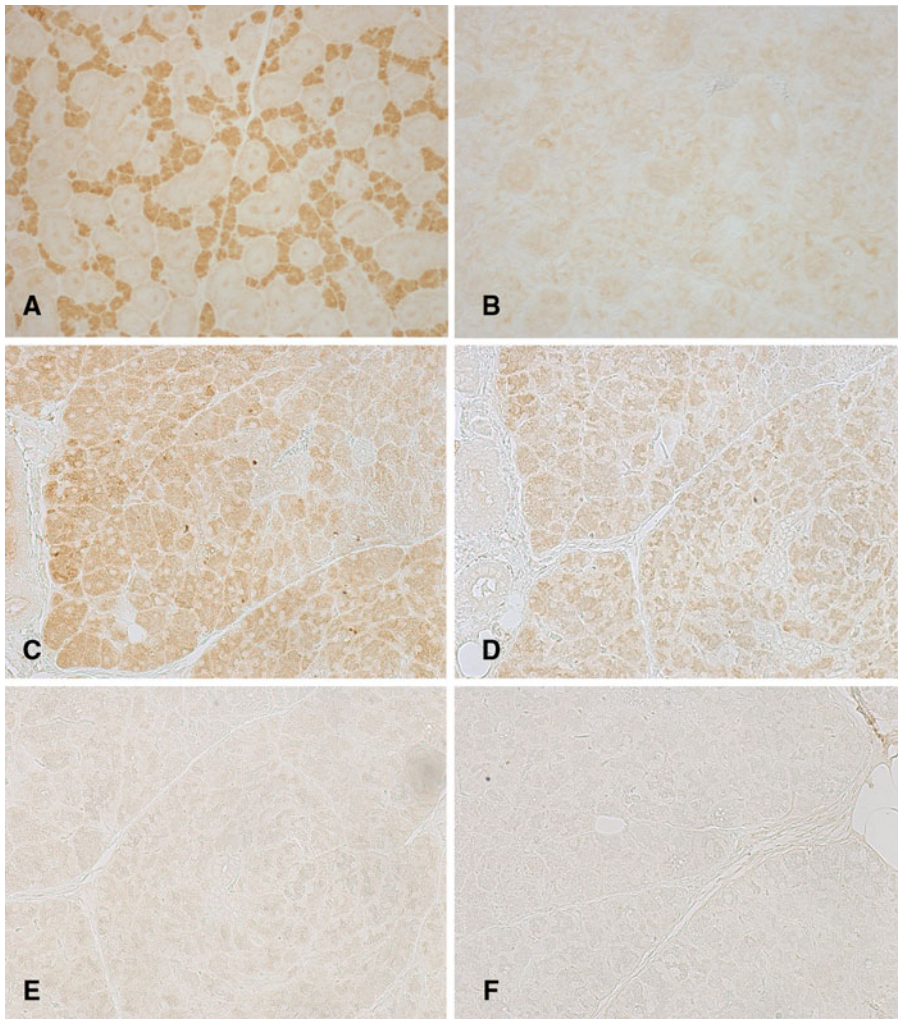

Fig. 3 Immunohistochemical staining of the CAVI protein in the submandibular and parotid glands of wild-type and *Car6*$^{-/-}$ mice. Submandibular gland sections from wild-type (**A**) and *Car6*$^{-/-}$ mice (**B**) immunostained with non-preabsorbed anti-CAVI serum. The section from the wild-type mouse shows strong staining in the serous acini. A parotid gland section from *Car6*$^{-/-}$ knockout mouse stained with non-preabsorbed anti-CAVI serum exhibits a weak positive signal (**C**). Immunostaining of *Car6*$^{-/-}$ parotid gland with anti-CAVI serum preabsorbed with purified CAVI also shows a weak reaction (**D**) whereas no signal is detectable when anti-CAVI serum is first preabsorbed using the cross-reactive 56-kDa protein (**E**). Immunostaining with normal rabbit serum is negative (**F**). Original magnification, ×200

42, respectively. In addition, 27 and 100 genes were induced and repressed in the duodenum of *Car6*$^{-/-}$ mice, respectively. Figure 5 shows that most of the genes with altered expression levels are unique in individual tissues. Only two genes (*Cfd* and *Klk1b4*) were regulated in all the three tissues. Moreover, the expression of three (*Myl1*, *Klk1b5*, and *Klk1b27*), four (*Actb*, *Acot1*, *Expi*, and *Scd1*), and five (BC048546, 2310057J18Rik, *Chac1*, *Klk1b11*, and *Usp18*) genes were changed both in the submandibular gland and stomach, stomach and duodenum, and submandibular gland and duodenum, respectively. Complete lists of genes exhibiting altered expression levels, including their symbols, gene descriptions, fold change, and *P*-value, are shown in Tables 4, 5, and 6.

Functional annotation of differentially transcribed genes in *Car6*$^{-/-}$ mice

Gene ontology (GO) assignments for differentially expressed genes in the submandibular gland, stomach,

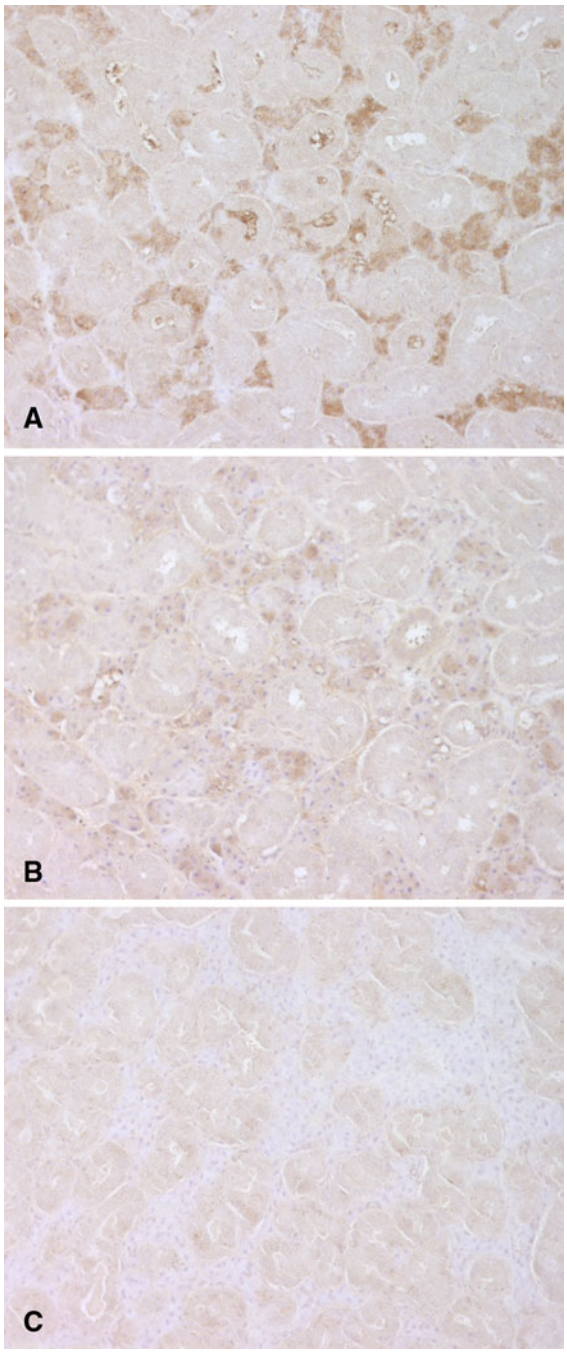

Fig. 4 Immunohistochemical staining of the CAVI protein in the submandibular gland of **A** wild-type, **B** *Car6*$^{+/-}$, and **C** *Car6*$^{-/-}$ mice, the intensity of staining varied from strong to none. Original magnification, ×200

and duodenum of *Car6*$^{-/-}$ mice were performed using the Visual Annotation Display (VLAD) tool. The analysis revealed significantly affected biological processes caused by CAVI deficiency in the above-mentioned tissues (Fig. 6).

The submandibular gland showed the highest number of altered biological processes of all tissues examined. Its genes involved in "metabolic process", especially "catabolic process" (e.g. the subclusters of "macromolecule catabolic process", "biopolymer catabolic process", "protein catabolic process", and "proteolysis"), "regulation of lipid metabolic process", "brown fat cell differentiation", and "response to oxidative stress" were significantly down-regulated. In contrast, the expression of genes involved in "negative regulation of gene-specific transcription from RNA polymerase II promoter" was increased in *Car6*$^{-/-}$ mice (Fig. 6A). The biological processes "phosphocreatine biosynthetic process" and "catabolic process" (by way of its subclusters "macromolecule catabolic process", "biopolymer catabolic process", "protein catabolic process", "proteolysis", and "digestion") were up- and down-regulated, respectively, in the stomach of *Car6*$^{-/-}$ mice (Fig. 6B). Notably, the biological processes "immune system process", "response to stress", and "Isg15-protein conjugation" were significantly induced while the "retinol metobolic process" was considerably repressed in the duodenum of *Car6*$^{-/-}$ mice (Fig. 6C). In contrast to the submandibular gland and stomach, the genes implicated in the "catabolic process" were found to be up-regulated in the duodenum.

Validation of differentially transcribed genes by qRT-PCR

In order to specifically analyze single genes, 16 transcriptionally altered genes (including *Car6*), detected by cDNA microarray, were evaluated by qRT-PCR. Among them, five genes were up- or down-regulated in the submandibular gland, whereas the expression levels of the remaining 11 genes were induced or repressed in the duodenum of *Car6*$^{-/-}$ mice. The altered expression levels of all 11 genes selected from the duodenum were confirmed accordingly, whereas three of the five genes from the submandibular gland were validated (Fig. 7A, B). The gene with the greatest alteration in transcription was identified as *Gast*, which is a gene encoding a hormone (gastrin) directly implicated in the secretion of gastric acid. *Gast* was confirmed by qRT-PCR to experience a

Table 2 Lymphoid follicles in Peyer's patches

Numbers of lymphoid follicles/patch	Wild-type	*Car6*$^{-/-}$	*P*-value
Male	4.21 ± 0.6 (n = 4)	5.99 ± 0.71 (n = 4)	0.009
Female	4.25 ± 0.77 (n = 6)	6.04 ± 0.6 (n = 5)	0.002

Table 3 pH values in the stomach and duodenum of wild-type and *Car6*$^{-/-}$ mice

pH value	Wild-type	*Car6*$^{-/-}$	*P*-value
Stomach	2.84 ± 0.55 (n = 8)	2.78 ± 0.64 (n = 4)	0.88
Duodenum	6.36 ± 0.40 (n = 8)	6.21 ± 0.09 (n = 4)	0.48

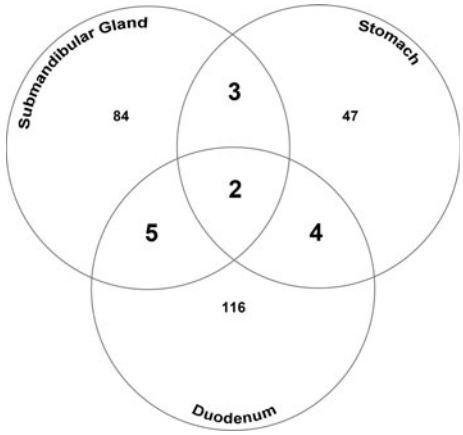

Fig. 5 Venn diagram of differentially expressed genes in the submandibular gland, stomach, and duodenum

15.1-fold decrease at the transcriptional level in the duodenum of *Car6*$^{-/-}$ mice. The fold changes of mRNA expression level confirmed by qRT-PCR for *Cldn18*, *Gif*, *Gkn1*, *Ly6g6e*, and *Spp1* were 5.8-fold, 9.2-fold, 5.1-fold, 5.3-fold, and 9-fold, respectively.

Importantly, several key players in the immune system response and ISG15-protein conjugation were found to be transcriptionally up-regulated in response to CAVI deficiency. We confirmed that three of these—namely, *Oasl2, Isg15*, and *Usp18*—were increased by 4.7-fold, 5.1-fold, and 7-fold, respectively.

Alterations in *Avil* and *Adh7* expression in the duodenum were confirmed by qRT-PCR. The results showed 5.3-fold and 8.2-fold decreases, respectively, in *Car6*$^{-/-}$ mice compared to the controls. *Avil* mRNA is highly expressed in the intestinal lining, the endometrium of the uterus, and the surface of the tongue in adult mice (Marks et al. 1998). It encodes the advillin protein, which belongs to the gelsolin/villin family of proteins, and may be involved in the morphogenesis of the microvilli (Tumer et al. 2002). Alcohol dehydrogenase 7 (ADH7), encoded by the *Adh7* gene, is one member of the alcohol-metabolizing enzyme family. It is uniquely expressed in the stomach mucosa where it influences the metabolism of alcohol prior to its absorption into the blood (Birley et al. 2008). ADH7 has been associated with certain cancers (Birley et al. 2008).

The dramatically decreased mRNA expression of *Car6* in the submandibular gland of *Car6*$^{-/-}$ mice further verified the successful disruption of the *Car6* gene, with a consequent reduction of the CAVI enzyme in these mice. Interestingly, *Car3* was confirmed by qRT-PCR to be down-regulated by 5.7-fold, which may partially contribute to the repression of the "response to oxidative stress" in the submandibular gland when performing GO assignment for differentially transcribed genes. The third gene induced by 4.7-fold in the submandibular gland was *Gcnt1*, which plays a critical role in lymphocyte trafficking during chronic inflammation (Hiraoka et al. 2004). In addition, the mRNA expression levels of *Alg5* and *Brf1* were found to be elevated for 2.3 and 2.14 times by cDNA microarray analyses. *Alg5* encodes the dolichyl phosphate glucosyltransferase, which participates in the glucosylation of the oligomannose core (Imbach et al. 1999). *Brf1* cDNA was originally cloned as an epidermal growth factor-inducible gene in rat intestinal epithelial cells (Stumpo et al. 2004). BRF1 protein posttranscriptionally regulates mRNA levels by targeting ARE-bearing transcript to the decay machinery (Benjamin et al. 2006). However, qRT-PCR results showed no significant change at the mRNA expression level of *Alg5* and *Brf1* between the wild-type and *Car6*$^{-/-}$ mice.

The expression levels of the same 16 genes in three male wild-type and three male *Car6*$^{-/-}$ mice were evaluated by qRT-PCR as well. Results summarized in Fig. 7C and D indicated that except for *Car6* and

Table 4 Genes differentially expressed in the submandibular gland of *Car6*$^{-/-}$ mice

Gene symbol	Description	FC	*P*-value
Gcnt1	Glucosaminyl (*N*-acetyl) transferase 1, core 2	5.18	0.0004
Pgk1	Phosphoglycerate kinase 1	3.88	0.0007
BC048546	cDNA sequence BC048546	3.20	0.004
Dcpp2	Demilune cell and parotid protein 2	2.76	0.006
Alg5	Asparagine-linked glycosylation 5 homolog (yeast, dolichyl-phosphate beta-glucosyltransferase)	2.30	0.009
Eno1	Enolase 1, alpha non-neuron	2.30	0.010
Dcpp1	Demilune cell and parotid protein 1	2.24	0.012
3300001G02Rik	RIKEN cDNA 3300001G02 gene	2.14	0.019
Brf1	BRF1 homolog, subunit of RNA polymerase III transcription initiation factor IIIB (S. cerevisiae)	2.14	0.028
Slc35c2	Solute carrier family 35, member C2	2.11	0.035
Psp	Parotid secretory protein	2.08	0.041
Dcpp3	Demilune cell and parotid protein 3	2.06	0.054
4930455C21Rik	RIKEN cDNA 4930455C21 gene	1.97	0.063
Clcnkb	Chloride channel Kb	1.95	0.090
Padi2	Peptidyl arginine deiminase, type II	1.95	0.098
Gnal	Guanine nucleotide binding protein, alpha stimulating, olfactory type	1.88	0.142
Irf1	Interferon regulatory factor 1	1.79	0.163
Oit1	Oncoprotein induced transcript 1	1.74	0.195
Scd2	Stearoyl-Coenzyme A desaturase 2	1.73	0.200
Sp2	Sp2 transcription factor	1.72	0.219
2310057J18Rik	RIKEN cDNA 2310057J18 gene	1.59	0.229
Kctd14	Potassium channel tetramerisation domain containing 14	1.58	0.445
Glrx	Glutaredoxin	1.55	0.552
Rrbp1	Ribosome binding protein 1	1.47	0.565
Per2	Period homolog 2 (Drosophila)	1.46	0.566
Per1	Period homolog 1 (Drosophila)	1.45	0.632
Golga2	Golgi autoantigen, golgin subfamily a, 2	1.44	0.648
Fah	Fumarylacetoacetate hydrolase	−1.42	0.270
1500012F01Rik	RIKEN cDNA 1500012F01 gene	−1.43	0.216
Gpx2	Glutathione peroxidase 2	−1.44	0.384
Cyp2a5	Cytochrome P450, family 2, subfamily a, polypeptide 5	−1.45	0.196
Myl1	Myosin, light polypeptide 1	−1.46	0.278
Pdk4	Pyruvate dehydrogenase kinase, isoenzyme 4	−1.46	0.183
Gstm1	Glutathione S-transferase, mu 1	−1.46	0.225
Hadhb	Hydroxyacyl-Coenzyme A dehydrogenase/3-ketoacyl-Coenzyme A thiolase/enoyl-Coenzyme A hydratase (trifunctional protein), beta subunit	−1.46	0.195
Slc25a20	Solute carrier family 25 (mitochondrial carnitine/acylcarnitine translocase), member 20	−1.48	0.210
S3-12	Plasma membrane associated protein, S3-12	−1.48	0.237
Car13	Carbonic anhydrase 13	−1.48	0.184
Cox8b	Cytochrome c oxidase, subunit VIIIb	−1.49	0.367
Cat	Catalase	−1.49	0.337
Fbxl3	F-box and leucine-rich repeat protein 3	−1.49	0.161

Table 4 continued

Gene symbol	Description	FC	*P*-value
St3gal6	ST3 beta-galactoside alpha-2,3-sialyltransferase 6	−1.50	0.349
Usp18	Ubiquitin specific peptidase 18	−1.50	0.156
Klk1b11	Kallikrein 1-related peptidase b11	−1.52	0.223
Egf	Epidermal growth factor	−1.53	0.276
Tspo	Translocator protein	−1.54	0.129
Rnase4	Ribonuclease, RNase A family 4	−1.55	0.15
Angptl4	Angiopoietin-like 4	−1.55	0.174
Hsd11b1	Hydroxysteroid 11-beta dehydrogenase 1	−1.56	0.112
Klk1b24	Kallikrein 1-related peptidase b24	−1.57	0.179
Pygl	Liver glycogen phosphorylase	−1.60	0.276
Klk1b27	Kallikrein 1-related peptidase b27	−1.61	0.195
Agpat2	1-Acylglycerol-3-phosphate O-acyltransferase 2 (lysophosphatidic acid acyltransferase, beta)	−1.61	0.195
Egfbp2	Epidermal growth factor binding protein type B	−1.62	0.111
Rnase1	Ribonuclease, RNase A family, 1 (pancreatic)	−1.62	0.261
Nnmt	Nicotinamide *N*-methyltransferase	−1.62	0.119
Serpinb6a	Serine (or cysteine) peptidase inhibitor, clade B, member 6a	−1.62	0.089
Klk1b22	Kallikrein 1-related peptidase b22	−1.62	0.173
Ces3	Carboxylesterase 3	−1.64	0.208
Klk1b16	Kallikrein 1-related peptidase b16	−1.65	0.223
Cidea	Cell death-inducing DNA fragmentation factor, alpha subunit-like effector A	−1.66	0.462
Mgst1	Microsomal glutathione S-transferase 1	−1.70	0.105
Dgat2	Diacylglycerol O-acyltransferase 2	−1.72	0.275
Gpx3	Glutathione peroxidase 3	−1.73	0.197
Hba-a1	Hemoglobin alpha, adult chain 1	−1.75	0.109
Mgst1	Microsomal glutathione S-transferase 1	−1.76	0.121
Klk1b1	Kallikrein 1-related peptidase b1	−1.77	0.166
Klk1b5	Kallikrein 1-related peptidase b5	−1.79	0.119
Snca	Synuclein, alpha	−1.80	0.129
Gsta3	Glutathione S-transferase, alpha 3	−1.81	0.135
Ucp1	Uncoupling protein 1 (mitochondrial, proton carrier)	−1.82	0.385
Mmd	Monocyte to macrophage differentiation-associated	−1.84	0.113
Cidec	Cell death-inducing DFFA-like effector c	−1.86	0.139
Klk1b9	Kallikrein 1-related peptidase b9	−1.88	0.138
Xlr4a	X-linked lymphocyte-regulated 4A	−1.88	0.127
Arg1	Arginase, liver	−1.88	0.044
Lpl	Lipoprotein lipase	−1.90	0.114
Klk1b8	Kallikrein 1-related peptidase b8	−1.94	0.090
Orm1	Orosomucoid 1	−1.94	0.082
Klk1b4	Kallikrein 1-related pepidase b4	−1.96	0.108
Klk1b21	Kallikrein 1-related peptidase b21	−2.04	0.140
Ngf	Nerve growth factor	−2.06	0.140
Cfd	Complement factor D (adipsin)	−2.06	0.132
Klk1b21	Kallikrein 1-related peptidase b21	−2.06	0.140

Table 4 continued

Gene symbol	Description	FC	*P*-value
BC054059	cDNA sequence BC054059	−2.07	0.125
Snca	Synuclein, alpha	−2.08	0.099
Thrsp	Thyroid hormone responsive SPOT14 homolog (Rattus)	−2.11	0.192
Car6	Carbonic anhydrase 6	−2.16	0.008
Tmem45b	Transmembrane protein 45b	−2.23	0.120
Adipoq	Adiponectin, C1Q and collagen domain containing	−2.32	0.082
Chac1	ChaC, cation transport regulator-like 1 (E. coli)	−2.33	0.156
Cyp2e1	Cytochrome P450, family 2, subfamily e, polypeptide 1	−2.34	0.110
Klk1b9	Kallikrein 1-related peptidase b9	−2.44	0.038
Car3	Carbonic anhydrase 3	−2.70	0.097

Table 5 Genes differentially expressed in the stomach of $Car6^{-/-}$ mice

Gene symbol	Description	FC	*P*-value
Myl1	Myosin, light polypeptide 1	2.78	0.284
Acta1	Actin, alpha 1, skeletal muscle	2.64	0.310
Tnnc2	Troponin C2, fast	2.38	0.365
Myl3	Myosin, light polypeptide 3	2.15	0.422
Mylpf	Myosin light chain, phosphorylatable, fast skeletal muscle	1.81	0.533
Defb4	Defensin beta 4	1.77	0.549
Mb	Myoglobin	1.70	0.575
Eno3	Enolase 3, beta muscle	1.68	0.583
2010109I03Rik	RIKEN cDNA 2010109I03 gene	1.65	0.600
Atp2a1	ATPase, Ca++ transporting, cardiac muscle, fast twitch 1	1.59	0.624
Tnnt1	Troponin T1, skeletal, slow	1.54	0.648
Tpm2	Tropomyosin 2, beta	1.54	0.650
Ckm	Creatine kinase, muscle	1.51	0.662
Myh8	Myosin, heavy polypeptide 8, skeletal muscle, perinatal	1.48	0.678
Cfd	Complement factor D (adipsin)	−1.42	0.710
Scd1	Stearoyl-Coenzyme A desaturase 1	−1.43	0.708
Tacstd2	Tumor-associated calcium signal transducer 2	−1.48	0.679
Acot1	Acyl-CoA thioesterase 1	−1.58	0.629
S100a8	S100 calcium binding protein A8 (calgranulin A)	−1.60	0.619
Sycn	Syncollin	−1.68	0.585
Retnlg	Resistin like gamma	−1.80	0.538
2210010C04Rik	RIKEN cDNA 2210010C04 gene	−1.81	0.531
Ear11	Eosinophil-associated, ribonuclease A family, member 11	−1.84	0.520
Actb	Actin, beta	−1.85	0.517
Expi	Extracellular proteinase inhibitor	−1.90	0.500
Chi3l4	Chitinase 3-like 4	−1.98	0.473
Prss2	Protease, serine, 2	−1.99	0.470
Mup5	Major urinary protein 5	−2.00	0.467
Klk1b26	Kallikrein 1-related petidase b26	−2.02	0.460
Cel	Carboxyl ester lipase	−2.03	0.458

Table 5 continued

Gene symbol	Description	FC	*P*-value
Reg3b	Regenerating islet-derived 3 beta	−2.08	0.444
Wfdc12	WAP four-disulfide core domain 12	−2.10	0.437
Cuzd1	CUB and zona pellucida-like domains 1	−2.23	0.400
Spink3	Serine peptidase inhibitor, Kazal type 3	−2.32	0.378
Ela1	Elastase 1, pancreatic	−2.36	0.367
Spt1	Salivary protein 1	−2.51	0.335
Amy2	Amylase 2, pancreatic	−2.65	0.307
Reg2	Regenerating islet-derived 2	−2.84	0.275
Ctrb1	Chymotrypsinogen B1	−2.94	0.259
Reg1	Regenerating islet-derived 1	−3.14	0.231
Klk1b27	Kallikrein 1-related peptidase b27	−3.25	0.217
Gp2	Glycoprotein 2 (zymogen granule membrane)	−3.34	0.207
Ela3	Elastase 3, pancreatic	−3.77	0.165
1190003M12Rik	RIKEN cDNA 1190003M12 gene	−3.88	0.156
Klk1b4	Kallikrein 1-related pepidase b4	−3.90	0.153
Ctrl	Chymotrypsin-like	−4.00	0.146
Klk1b5	Kallikrein 1-related peptidase b5	−4.30	0.127
Klk1	Kallikrein 1	−4.57	0.112
Pnlip	Pancreatic lipase	−5.05	0.090
Pip	Prolactin induced protein	−5.25	0.083
1810010M01Rik	RIKEN cDNA 1810010M01 gene	−5.36	0.079
Abpb	Androgen binding protein beta	−6.04	0.060
Muc10	Mucin 10, submandibular gland salivary mucin	−6.08	0.059
RP23-395H4.4	Elastase 2A	−7.36	0.037
Abpa	Androgen binding protein alpha	−7.78	0.032
Abpg	Androgen binding protein gamma	−9.40	0.019

Table 6 Genes differentially expressed in the duodenum of *Car6*$^{-/-}$ mice

Gene symbol	Description	FC	*P*-value
Isg15	ISG15 ubiquitin-like modifier	5.31	0.008
Usp18	Ubiquitin specific peptidase 18	4.99	0.011
Oasl2	2-5 Oligoadenylate synthetase-like 2	4.97	0.011
Igtp	Interferon gamma induced GTPase	4.76	0.014
Ubd	Ubiquitin D	4.02	0.028
Oas1 g	2-5 Oligoadenylate synthetase 1G	3.53	0.047
Ang4	Angiogenin, ribonuclease A family, member 4	3.26	0.062
Rsad2	Radical S-adenosyl methionine domain containing 2	3.18	0.068
Irgm1	Immunity-related GTPase family M member 1	3.13	0.072
Slc13a2	Solute carrier family 13 (sodium-dependent dicarboxylate transporter), member 2	3.05	0.078
Indo	Indoleamine-pyrrole 2,3 dioxygenase	3.03	0.081
Psmb9	Proteasome (prosome, macropain) subunit, beta type 9 (large multifunctional peptidase 2)	2.99	0.084

Table 6 continued

Gene symbol	Description	FC	*P*-value
Iigp2	Interferon inducible GTPase 2	2.97	0.086
Dnase1	Deoxyribonuclease I	2.96	0.089
Ifi47	Interferon gamma inducible protein 47	2.82	0.102
Lyz1	Lysozyme 1	2.70	0.118
H2-DMa	Histocompatibility 2, class II, locus DMa	2.59	0.133
2010204N08Rik	RIKEN cDNA 2010204N08 gene	2.56	0.139
H2-Ab1	Histocompatibility 2, class II antigen A, beta 1	2.56	0.139
St3 gal4	ST3 beta-galactoside alpha-2,3-sialyltransferase 4	2.41	0.166
Mep1b	Meprin 1 beta	2.39	0.169
Defcr5	Defensin related cryptdin 5	2.38	0.171
Defcr26	Defensin related cryptdin 26	2.37	0.173
Reg3 g	Regenerating islet-derived 3 gamma	2.02	0.266
Defcr-rs1	Defensin related sequence cryptdin peptide (paneth cells)	1.98	0.282
H2-Aa	Histocompatibility 2, class II antigen A, alpha	1.72	0.389
Ccl5	Chemokine (C–C motif) ligand 5	1.66	0.421
AI428936	Expressed sequence AI428936	−1.52	0.506
Serpina10	Serine (or cysteine) peptidase inhibitor, clade A (alpha-1 antiproteinase, antitrypsin), member 10	−1.55	0.487
Rbpjl	Recombination signal binding protein for immunoglobulin kappa J region-like	−1.62	0.443
Cldn10	Claudin 10	−1.63	0.441
Gnmt	Glycine *N*-methyltransferase	−1.63	0.441
Erp27	Endoplasmic reticulum protein 27	−1.67	0.415
Prss3	Protease, serine, 3	−1.70	0.403
Aqp12	Aquaporin 12	−1.70	0.403
Chac1	ChaC, cation transport regulator-like 1 (E. coli)	−1.70	0.403
Arhgdig	Rho GDP dissociation inhibitor (GDI) gamma	−1.76	0.375
Hba-a1	Hemoglobin alpha, adult chain 1	−1.77	0.367
Hamp2	Hepcidin antimicrobial peptide 2	−1.80	0.352
Cabp2	Calcium binding protein 2	−1.81	0.348
Actb	Actin, beta	−1.81	0.307
Klk1b11	Kallikrein 1-related peptidase b11	−1.92	0.305
Slc38a5	Solute carrier family 38, member 5	−1.93	0.300
Klk1b4	Kallikrein 1-related pepidase b4	−2.02	0.266
Ltf	Lactotransferrin	−2.03	0.264
Atp4b	ATPase, H +/K + exchanging, beta polypeptide	−2.10	0.240
Ern2	Endoplasmic reticulum (ER) to nucleus signalling 2	−2.19	0.216
Gal	Galanin	−2.21	0.211
Fgf21	Fibroblast growth factor 21	−2.29	0.192
1810009J06Rik	RIKEN cDNA 1810009J06 gene	−2.54	0.144
Hmgcs2	3-Hydroxy-3-methylglutaryl-Coenzyme A synthase 2	−2.61	0.130
Chia	Chitinase, acidic	−2.65	0.125
Acot1	Acyl-CoA thioesterase 1	−2.66	0.123
Clu	Clusterin	−2.69	0.119
BC048546	cDNA sequence BC048546	−2.69	0.119

Table 6 continued

Gene symbol	Description	FC	*P*-value
Cmtm8	CKLF-like MARVEL transmembrane domain containing 8	−2.74	0.112
Adam28	A disintegrin and metallopeptidase domain 28	−2.74	0.112
Cfd	Complement factor D (adipsin)	−2.77	0.108
Capn13	Calpain 13	−2.78	0.107
Scara3	Scavenger receptor class A, member 3	−2.84	0.099
Efna5	Ephrin A5	−2.87	0.096
Azgp1	Alpha-2-glycoprotein 1, zinc	−2.90	0.093
Ttc39a	Tetratricopeptide repeat domain 39A	−2.91	0.092
Ttr	Transthyretin	−2.92	0.091
Sftpd	Surfactant associated protein D	−2.92	0.091
Scd1	Stearoyl-Coenzyme A desaturase 1	−2.93	0.090
Chad	Chondroadherin	−2.94	0.008
Chia	Chitinase, acidic	−2.94	0.008
Tesc	Tescalcin	−3.00	0.083
Rpp25	Ribonuclease P 25 subunit (human)	−3.01	0.082
Ctse	Cathepsin E	−3.04	0.079
Sytl1	Synaptotagmin-like 1	−3.06	0.078
Shh	Sonic hedgehog	−3.07	0.077
Fut2	Fucosyltransferase 2	−3.10	0.074
Expi	Extracellular proteinase inhibitor	−3.10	0.074
Lypd6b	LY6/PLAUR domain containing 6B	−3.11	0.073
Tst	Thiosulfate sulfurtransferase, mitochondrial	−3.11	0.073
Syt8	Synaptotagmin VIII	−3.13	0.072
Muc1	Mucin 1, transmembrane	−3.16	0.069
Aqp5	Aquaporin 5	−3.21	0.066
Rab27a	RAB27A, member RAS oncogene family	−3.32	0.058
Krt23	Keratin 23	−3.38	0.055
2310042E22Rik	RIKEN cDNA 2310042E22 gene	−3.38	0.055
Bcas1	Breast carcinoma amplified sequence 1	−3.43	0.052
Slc45a3	Solute carrier family 45, member 3	−3.47	0.050
Wfdc2	WAP four-disulfide core domain 2	−3.47	0.050
Fxyd3	FXYD domain-containing ion transport regulator 3	−3.48	0.049
Gldc	Glycine decarboxylase	−3.52	0.049
Muc6	Mucin 6, gastric	−3.53	0.046
Anxa3	Annexin A3	−3.54	0.046
Ly6g6e	Lymphocyte antigen 6 complex, locus G6E	−3.56	0.045
Bace2	Beta-site APP-cleaving enzyme 2	−3.58	0.044
Vsig2	V-set and immunoglobulin domain containing 2	−3.67	0.040
Anxa3	Annexin A3	−3.68	0.040
Rbp1	Retinol binding protein 1, cellular	−3.72	0.038
Vsig2	V-set and immunoglobulin domain containing 2	−3.76	0.037
Cbr3	Carbonyl reductase 3	−3.77	0.036
Tff1	Trefoil factor 1	−3.78	0.036
Sult1c2	Sulfotransferase family, cytosolic, 1C, member 2	−3.93	0.031
Aqp5	Aquaporin 5	−4.00	0.028

Table 6 continued

Gene symbol	Description	FC	*P*-value
Akr1b8	Aldo–keto reductase family 1, member B8	−4.12	0.025
Syt16	Synaptotagmin XVI	−4.16	0.024
Avil	Advillin	−4.25	0.022
2310057J18Rik	RIKEN cDNA 2310057J18 gene	−4.27	0.022
Ly6g6c	Lymphocyte antigen 6 complex, locus G6C	−4.90	0.012
Pgc	progastricsin (pepsinogen C)	−4.95	0.011
C130090K23Rik	RIKEN cDNA C130090K23 gene	−5.02	0.011
Adh7	Alcohol dehydrogenase 7 (class IV), mu or sigma polypeptide	−5.12	0.010
Spp1	Secreted phosphoprotein 1	−5.16	0.009
Vstm2b	V-set and transmembrane domain containing 2B	−5.82	0.005
Sox21	SRY-box containing gene 21	−5.86	0.005
Aldh3a1	Aldehyde dehydrogenase family 3, subfamily A1	−6.09	0.004
Mup2	Major urinary protein 2	−6.58	0.003
Gkn1	Gastrokine 1	−6.85	0.002
Mal	Myelin and lymphocyte protein, T-cell differentiation protein	−6.90	0.002
620807	Predicted gene, 620807	−7.02	0.002
Gkn2	Gastrokine 2	−7.04	0.002
Gldc	Glycine decarboxylase	−7.06	0.002
Cldn18	Claudin 18	−7.11	0.002
Gif	Gastric intrinsic factor	−7.98	0.0001
Gsdma2	Gasdermin A2	−8.57	0.0007
Dpcr1	Diffuse panbronchiolitis critical region 1 (human)	−9.16	0.0004
Mup2	Major urinary protein 2	−10.68	0.0001
Muc5ac	Mucin 5, subtypes A and C, tracheobronchial/gastric	−11.31	0.0001
Psapl1	Prosaposin-like 1	−11.52	0.0001
Psca	Prostate stem cell antigen	−12.24	8.20E−05
Mup1	Major urinary protein 1	−14.12	3.10E−05
Gast	Gastrin	−15.56	1.60E−05

Car3, the altered expression levels of the rest genes were somehow different from that of females, suggesting the gender effect at genomic level.

Besides, to determine whether loss of function of CAVI in the knockout mouse models leads to compensatory changes in other CAs, the mRNA expression of all 13 enzymatically active CAs in three wild-type and *Car6*$^{-/-}$ female mice was evaluated by qRT-PCR (Fig. 8). The results show that no such compensatory changes were detected.

Discussion

The present study describes, for the first time, the generation and phenotype of CAVI knockout mice. Immunohistochemical and immunoblotting analyses of salivary glands showed that CAVI was absent in *Car6*$^{-/-}$ mice indicating that the *Car6* gene had been successfully disrupted. However, the expression of CAVI was detected in the heterozygous *Car6*$^{+/-}$ mice, although the amount of protein was less as compared to wild-type mice. A cDNA microarray analysis and subsequent qRT-PCR of the RNA samples purified from the submandibular gland further confirmed the absence of *Car6* mRNA in *Car6*$^{-/-}$ mice. The growth, fertility, and life span of the mutant mice were similar to the wild-type control mice. No morphological differences were found between knockout and wild-type mice in the salivary, lacrimal, or mammary glands, all of which are known to secrete CAVI (data not shown). This result

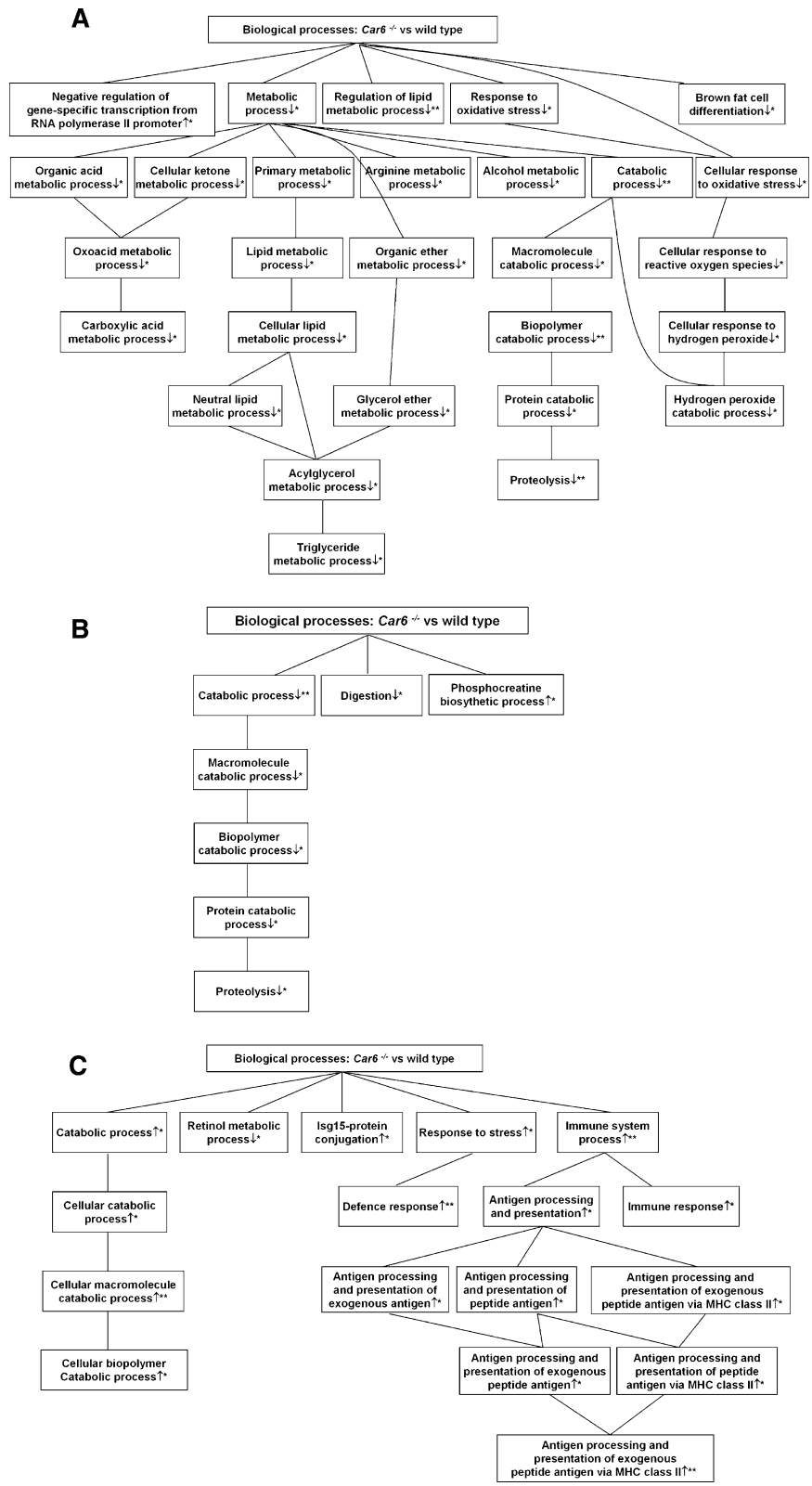

Fig. 6 Gene Ontology "Biological process" annotation results for differentially transcribed genes in tissues of *Car6*$^{-/-}$ mice. **A** Submandibular gland; **B** stomach; **C** duodenum; ↓: repressed biological processes; ↑: induced biological processes; *: processes meet the pruning threshold; **: processes meet both the pruning threshold and the collapsing threshold

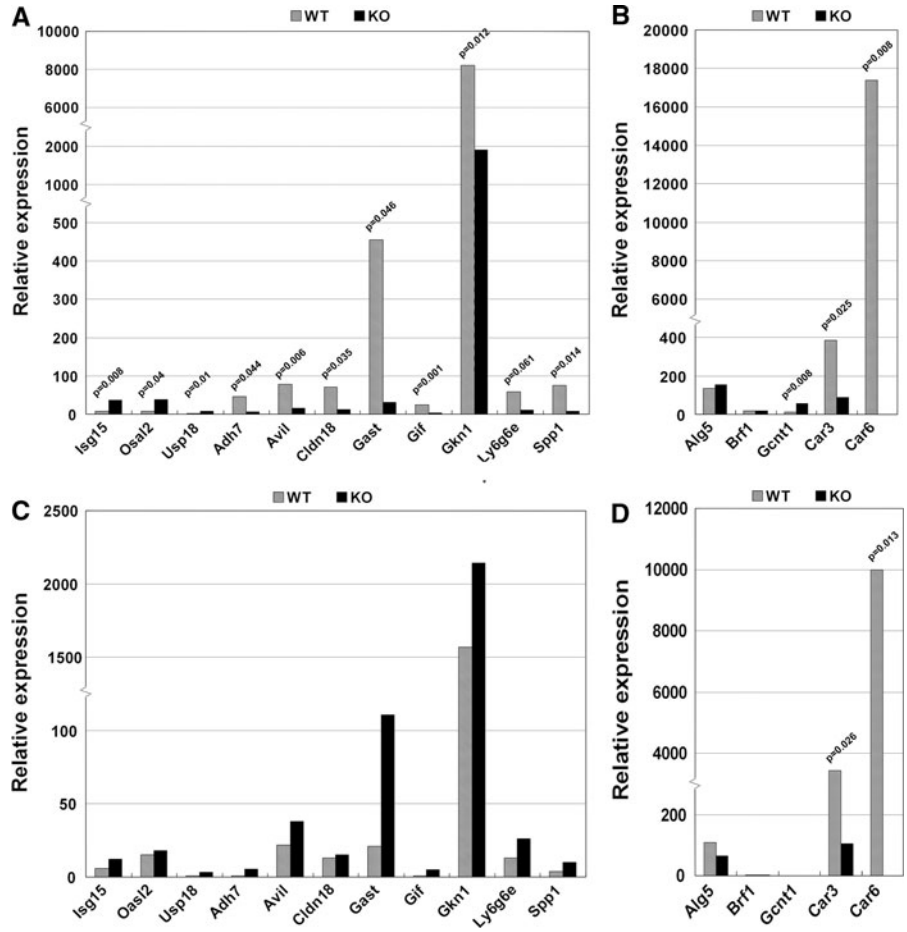

Fig. 7 qRT-PCR of differentially expressed genes in female and male mice. Genes in **A** duodenum and **B** submandibular gland of female mice and genes in **C** duodenum and **D** submandibular gland of male mice. WT: wild-type mice; KO: *Car6*$^{-/-}$ mice. *P*-values were indicated for genes of significant changes

suggests that CAVI, as a secreted isoenzyme, is not involved in intracrine morphological regulation in these exocrine glands.

CAVI is delivered to the alimentary tract in large amounts in saliva and particularly in colostral milk (Karhumaa et al. 2001). Recent studies have provided evidence that this isozyme helps to protect the teeth from caries (Kivela et al. 1999) and to neutralize the acid within the mucus layer covering the respiratory, esophageal, and gastric epithelia (Leinonen et al. 2004; Parkkila et al. 1997). The *Car6*$^{-/-}$ mice showed no obvious differences from the wild-type mice in teeth morphology or epithelial structures of the respiratory and gastrointestinal tracts (data not shown). In future studies, the *Car6*$^{-/-}$ mice will be exposed to dental caries induced by *Streptococcus mutans* inoculation and a high-sucrose diet. This experiment should undoubtedly reveal whether CAVI plays a role in preventing the formation of dental caries.

In order to characterize the effect of CAVI deficiency on gene expression profiles and biological processes, the transcriptomes of the submandibular gland, stomach, and duodenum from *Car6*$^{-/-}$ mice were analyzed and compared to the wild-type transcriptomes by cDNA microarray analysis. Analyzing of the data using Chipster^{TM} software revealed 94, 56, and 127 genes were up- or down-regulated in the submandibular gland, stomach, and duodenum of *Car6*$^{-/-}$ mice, respectively. Functional clustering of these differentially transcribed genes according to GO categories showed that many biological processes were significantly affected by the deficiency of CAVI. Notably, catabolic processes were repressed in both the submandibular gland and stomach, but induced in the duodenum. The alteration of this particular biological process in all three tissues of *Car6*$^{-/-}$ mice suggests that CAVI may be functionally involved - probably indirectly - in catabolism.

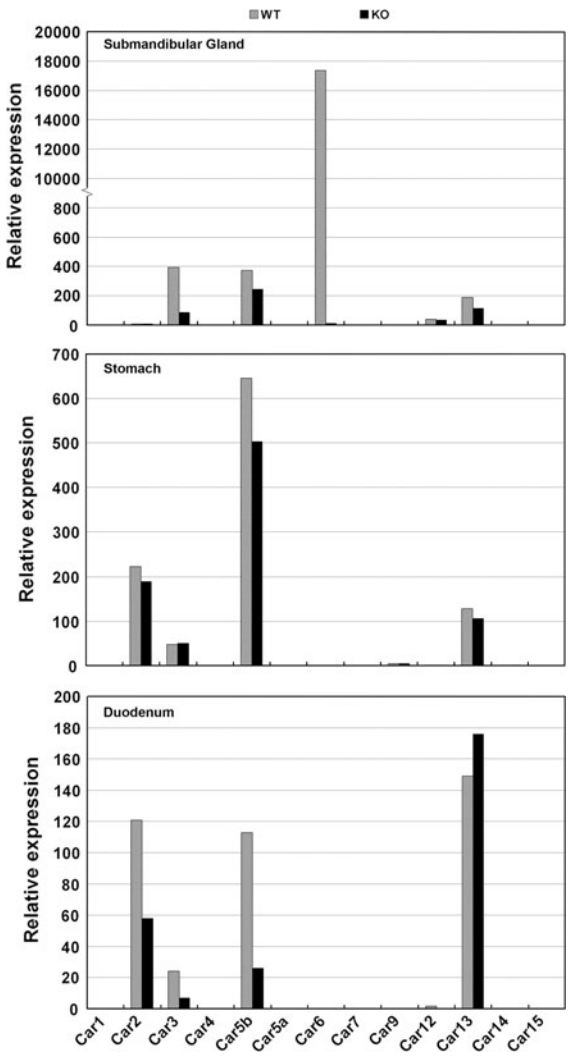

Fig. 8 qRT-PCR of carbonic anhydrases in females. WT: wild-type mice; KO: *Car6*$^{-/-}$ mice

In contrast to its isozymes, CAVI is not significantly expressed in the gastrointestinal tract epithelia (Pan et al. 2007; Parkkila et al. 1994). It is delivered in saliva and milk to the alimentary tract where it may protect gastric epithelium from acid injury and promote growth under certain abnormal physiological condition (Karhumaa et al. 2001; Parkkila et al. 1997). CAVI concentration is relatively high in both saliva and milk. Approximately 7–10 mg of acid-resistant salivary CAVI is swallowed daily into the gastrointestinal tract (Parkkila et al. 1993). It has been suggested that CAVI and CAII form a complementary system for the rapid removal of excess acidity from mucosal surfaces; specifically, CAVI may function as an acid neutralizer (whereas CA II is a bicarbonate producer) by catalyzing the reaction $HCO_3^- + H^+ \rightarrow CO_2 + H_2O$ (Parkkila et al. 1990). Histology of the gastrointestinal mucosa of *Car6*$^{-/-}$ mice did not differ from that of wild-type mice, which suggests that within the liquid phase of the gastric mucus neutralization is probably rapid enough even in the absence of the enzyme. The cDNA microarray analysis and qRT-PCR results revealed clear transcriptional repression of several genes implicated in the secretion and function of the gastric fluid. First of all, the most transcriptionally repressed gene detected in the duodenum of *Car6*$^{-/-}$ mice was *Gast*. This gene encodes a liner peptide hormone, namely gastrin, which is released by G cells of the stomach and duodenum into the bloodstream. Gastrin stimulates the secretion of gastric acid by the parietal cells of the stomach (Schubert 2008). The release of gastrin is inhibited by the presence of acid in the stomach. When there is no CAVI in the saliva to be supplied to the gastrointestinal tract of *Car6*$^{-/-}$ mice, less acid may be consequently secreted to prevent the accumulation of excess acid, therefore the pH value in the stomach of *Car6*$^{-/-}$ mice remains same as normal. Our results obtained from pH measurement in the stomach and duodenum of control and *Car6*$^{-/-}$ mice strengthen this speculation. The secretion of the gastric intrinsic factor, a protein encoded by *GIF*, also down-regulated in the duodenum of *Car6*$^{-/-}$ mice, is stimulated via all pathways known to stimulate gastric acid secretion (Nomura et al. 2005). It is not surprising that a decrease in *Gast* expression leads to the suppression of the *GIF* gene. Gastrokine 1 (Gkn1) has been reported to be highly expressed in normal stomach where it is located in the superficial/foveolar gastric epithelium, but it is absent from gastric carcinomas. The function of gastrokine 1 is unknown, but a role in mucosal protection has been postulated (Oien et al. 2004). In our study, the mRNA expression level of *Gkn1* was down-regulated significantly. This result could indicate that when less acid is secreted due to decreased *Gast* expression, there may be less induction of protective mechanisms within the gastric mucosa. A similar reason may as well account for the down-regulation of *Cldn18*, a gene encoding claudin 18, which is a member of the multigene family of claudins. Claudin 18 is the

dominant claudin in the tight junctions of specialized columnar epithelia and it has been suggested to contribute to greater acid resistance in Barrett's esophagus (Jovov et al. 2007).

We generated *Car6*$^{-/-}$ mice to study the physiological function of the CAVI enzyme. The gene disruption was successful as determined by western blots, immunohistochemical staining, and qRT-PCR results. The overall morphological phenotype in *Car6*$^{-/-}$ mice appears to be normal except for an increase in the number of lymphoid follicles in intestinal Peyer's patches. This finding suggests that a lack of CAVI in milk and saliva increases the permeability of the mucosa potentially causing an increased activity of the immune system in the intestinal area, which is consistent with the functional annotation result of up-regulated genes in the duodenum of *Car6*$^{-/-}$ mice detected via cDNA microarray analysis. Moreover, qRT-PCR results confirmed alterations in the mRNA expression levels of the three most predominantly induced genes. Among them, *ISG15* (ISG15 ubiquitin-like modifier) was originally characterized three decades ago as an interferon-stimulated gene (ISG) and its expression is highly induced upon interferon treatment (Kim and Zhang 2003). An elevated expression of ISG15 has also been detected in most cell types when infected with viruses or bacteria. It can be conjugated to various proteins in a similar manner as ubiquitin (Liu et al. 2005). Usp18 (ubiquitin specific peptidase 18, also known as Ubp43), is an Isg15-specific protease that is up-regulated in response to interferon or lipopolysaccaride. Its gene expression is required for normal Isg15 expression (Rempel et al. 2007). *Oasl2* (2′-5′ oligoadenylate synthetase-like 2), the third most predominantly up-regulated gene in the duodenum of *Car6*$^{-/-}$ mice, is an allergy/inflammation-related gene belonging to the 2′-5′ oligoadenylate synthetase family, which was one of the first characterized IFN-induced antiviral proteins (Eskildsen et al. 2003). Its expression is known to be induced in allergic contact dermatitis and skin sensitization (Ku et al. 2009). Up-regulation of the genes involved in the immunity suggests that a lack of postnatal breastfeeding or low CAVI content in milk and saliva may result in increased mucosal permeability that promotes the development of food allergies.

In conclusion, herein we describe the generation and use of *Car6*$^{-/-}$ mice to study the physiological function of the CAVI enzyme. The effects of CAVI deficiency on gene transcription were investigated using cDNA microarray analysis. *Car6*$^{-/-}$ mice had a greater number of lymphoid follicles in intestinal Peyer's patches compared with wild-type mice, which suggests that the lack of CAVI in colostral milk increases the permeability of the mucosa, potentially causing increased activity of the immune system in the intestinal area. Consistent with this speculation, the functional clustering of up-regulated genes detected by the cDNA microarray in the duodenum of *Car6*$^{-/-}$ mice revealed an induction of the immune system process. Using qRT-PCR, we demonstrated the up-regulations of three genes involved in the immune system response and ISG15-protein conjugation. Analysis of the transcriptomic patterns between wild-type and *Car6*$^{-/-}$ mice also revealed that the genes important in the catabolic processes were down-regulated in both the submandibular gland and stomach, although they were up-regulated in the duodenum. These results may reflect a functional role for CAVI in catabolic processes.

Acknowledgments The authors thank Zahid Shah, PhD, for valuable help in the construction of the targeting vector, and Alejandra Rodriguez Martinez, PhD, Marja Paloniemi, and the Biocenter Oulu Transgenic Core Facility for the technical assistance. This work was supported by grants from the Academy of Finland, the EU Framework 6 program (DeZnIT), and the Medical Fund of the Tampere University Hospital (9L071).

References

Amasaki H, Arai R, Ogawa M, Takemura N, Yamagami T, Nagasao J, Mutoh K, Ichihara N, Asari M (2003) Postnatal development of the mouse volatile papilla taste bud cells. J Vet Med Sci 65:541–543

Benjamin D, Schmidlin M, Min L, Gross B, Moroni C (2006) BRF1 protein turnover and mRNA decay activity are regulated by protein kinase B at the same phosphorylation sites. Mol Cell Biol 26:9497–9507

Birley AJ, James MR, Dickson PA, Montgomery GW, Heath AC, Whitfield JB, Martin NG (2008) Association of the gastric alcohol dehydrogenase gene ADH7 with variation in alcohol metabolism. Hum Mol Genet 17:179–189

Eskildsen S, Justesen J, Schierup MH, Hartmann R (2003) Characterization of the 2′-5′-oligoadenylate synthetase ubiquitin-like family. Nucleic Acids Res 31:3166–3173

Fernley RT, Wright RD, Coghlan JP (1979) A novel carbonic anhydrase from the ovine parotid gland. FEBS Lett 105:299–302

Fujikawa-Adachi K, Nishimori I, Sakamoto S, Morita M, Onishi S, Yonezawa S, Hollingsworth MA (1999)

Identification of carbonic anhydrase IV and VI mRNA expression in human pancreas and salivary glands. Pancreas 18:329–335

Gut MO, Parkkila S, Vernerova Z, Rohde E, Zavada J, Hocker M, Pastorek J, Karttunen T, Gibadulinova A, Zavadova Z, Knobeloch KP, Wiedenmann B, Svoboda J, Horak I, Pastorekova S (2002) Gastric hyperplasia in mice with targeted disruption of the carbonic anhydrase gene Car9. Gastroenterology 123:1889–1903

Henkin RI, Martin BM, Agarwal RP (1999) Efficacy of exogenous oral zinc in treatment of patients with carbonic anhydrase VI deficiency. Am J Med Sci 318:392–405

Hilvo M, Tolvanen M, Clark A, Shen B, Shah GN, Waheed A, Halmi P, Hanninen M, Hamalainen JM, Vihinen M, Sly WS, Parkkila S (2005) Characterization of CA XV, a new GPI-anchored form of carbonic anhydrase. Biochem J 392:83–92

Hiraoka N, Kawashima H, Petryniak B, Nakayama J, Mitoma J, Marth JD, Lowe JB, Fukuda M (2004) Core 2 branching beta1, 6-N-acetylglucosaminyltransferase and high endothelial venule-restricted sulfotransferase collaboratively control lymphocyte homing. J Biol Chem 279:3058–3067

Imbach T, Burda P, Kuhnert P, Wevers RA, Aebi M, Berger EG, Hennet T (1999) A mutation in the human ortholog of the Saccharomyces cerevisiae ALG6 gene causes carbohydrate-deficient glycoprotein syndrome type-Ic. Proc Natl Acad Sci USA 96:6982–6987

Jovov B, Van Itallie CM, Shaheen NJ, Carson JL, Gambling TM, Anderson JM, Orlando RC (2007) Claudin-18: a dominant tight junction protein in Barrett's esophagus and likely contributor to its acid resistance. Am J Physiol Gastrointest Liver Physiol 293:G1106–G1113

Karhumaa P, Leinonen J, Parkkila S, Kaunisto K, Tapanainen J, Rajaniemi H (2001) The identification of secreted carbonic anhydrase VI as a constitutive glycoprotein of human and rat milk. Proc Natl Acad Sci USA 98:11604–11608

Kaseda M, Ichihara N, Nishita T, Amasaki H, Asari M (2006) Immunohistochemistry of the bovine secretory carbonic anhydrase isozyme (CA-VI) in bovine alimentary canal and major salivary glands. J Vet Med Sci 68:131–135

Kasuya T, Shibata S, Kaseda M, Ichihara N, Nishita T, Murakami M, Asari M (2007) Immunohistolocalization and gene expression of the secretory carbonic anhydrase isozymes (CA-VI) in canine oral mucosa, salivary glands and oesophagus. Anat Histol Embryol 36:53–57

Kim KI, Zhang DE (2003) ISG15, not just another ubiquitin-like protein. Biochem Biophys Res Commun 307:431–434

Kim G, Lee TH, Wetzel P, Geers C, Robinson MA, Myers TG, Owens JW, Wehr NB, Eckhaus MW, Gros G, Wynshaw-Boris A, Levine RL (2004) Carbonic anhydrase III is not required in the mouse for normal growth, development, and life span. Mol Cell Biol 24:9942–9947

Kimoto M, Iwai S, Maeda T, Yura Y, Fernley RT, Ogawa Y (2004) Carbonic anhydrase VI in the mouse nasal gland. J Histochem Cytochem 52:1057–1062

Kimoto M, Kishino M, Yura Y, Ogawa Y (2006) A role of salivary carbonic anhydrase VI in dental plaque. Arch Oral Biol 51:117–122

Kivela J, Parkkila S, Waheed A, Parkkila AK, Sly WS, Rajaniemi H (1997) Secretory carbonic anhydrase isoenzyme (CA VI) in human serum. Clin Chem 43:2318–2322

Kivela J, Parkkila S, Parkkila AK, Rajaniemi H (1999) A low concentration of carbonic anhydrase isoenzyme VI in whole saliva is associated with caries prevalence. Caries Res 33:178–184

Kivela AJ, Parkkila S, Saarnio J, Karttunen TJ, Kivela J, Parkkila AK, Bartosova M, Mucha V, Novak M, Waheed A, Sly WS, Rajaniemi H, Pastorekova S, Pastorek J (2005) Expression of von Hippel-Lindau tumor suppressor and tumor-associated carbonic anhydrases IX and XII in normal and neoplastic colorectal mucosa. World J Gastroenterol 11:2616–2625

Ku HO, Jeong SH, Kang HG, Pyo HM, Cho JH, Son SW, Yun SM, Ryu DY (2009) Gene expression profiles and pathways in skin inflammation induced by three different sensitizers and an irritant. Toxicol Lett 190:231–237

Laemmli UK (1970) Cleavage of structural proteins during the assembly of the head of bacteriophage T4. Nature 227:680–685

Lehtonen J, Shen B, Vihinen M, Casini A, Scozzafava A, Supuran CT, Parkkila AK, Saarnio J, Kivela AJ, Waheed A, Sly WS, Parkkila S (2004) Characterization of CA XIII, a novel member of the carbonic anhydrase isozyme family. J Biol Chem 279:2719–2727

Leinonen J, Parkkila S, Kaunisto K, Koivunen P, Rajaniemi H (2001) Secretion of carbonic anhydrase isoenzyme VI (CA VI) from human and rat lingual serous von Ebner's glands. J Histochem Cytochem 49:657–662

Leinonen JS, Saari KA, Seppanen JM, Myllyla HM, Rajaniemi HJ (2004) Immunohistochemical demonstration of carbonic anhydrase isoenzyme VI (CA VI) expression in rat lower airways and lung. J Histochem Cytochem 52:1107–1112

Leppilampi M, Parkkila S, Karttunen T, Gut MO, Gros G, Sjoblom M (2005) Carbonic anhydrase isozyme-II-deficient mice lack the duodenal bicarbonate secretory response to prostaglandin E2. Proc Natl Acad Sci USA 102:15247–15252

Lewis SE, Erickson RP, Barnett LB, Venta PJ, Tashian RE (1988) N-ethyl-N-nitrosourea-induced null mutation at the mouse Car-2 locus: an animal model for human carbonic anhydrase II deficiency syndrome. Proc Natl Acad Sci USA 85:1962–1966

Liu YC, Penninger J, Karin M (2005) Immunity by ubiquitylation: a reversible process of modification. Nat Rev Immunol 5:941–952

Liu M, Walter GA, Pathare NC, Forster RE, Vandenborne K (2007) A quantitative study of bioenergetics in skeletal muscle lacking carbonic anhydrase III using 31P magnetic resonance spectroscopy. Proc Natl Acad Sci USA 104:371–376

Marks PW, Arai M, Bandura JL, Kwiatkowski DJ (1998) Advillin (p92): a new member of the gelsolin/villin family of actin regulatory proteins. J Cell Sci 111(Pt 15):2129–2136

Morey JS, Ryan JC, Van Dolah FM (2006) Microarray validation: factors influencing correlation between oligonucleotide microarrays and real-time PCR. Biol Proced Online 8:175–193

Murakami H, Sly WS (1987) Purification and characterization of human salivary carbonic anhydrase. J Biol Chem 262:1382–1388

Murakami M, Kasuya T, Matsuba C, Ichihara N, Nishita T, Fujitani H, Asari M (2003) Nucleotide sequence and expression of a cDNA encoding canine carbonic anhydrase VI (CA-VI). DNA Seq 14:195–198

Nezu A, Morita T, Tanimura A, Tojyo Y (2002) Comparison of amylase mRNAs from rat parotid gland, pancreas and liver using reverse transcriptase-polymerase chain reaction. Arch Oral Biol 47:563–566

Nomura S, Yamaguchi H, Ogawa M, Wang TC, Lee JR, Goldenring JR (2005) Alterations in gastric mucosal lineages induced by acute oxyntic atrophy in wild-type and gastrin-deficient mice. Am J Physiol Gastrointest Liver Physiol 288:G362–G375

Ogawa Y, Matsumoto K, Maeda T, Tamai R, Suzuki T, Sasano H, Fernley RT (2002) Characterization of lacrimal gland carbonic anhydrase VI. J Histochem Cytochem 50:821–827

Ogilvie JM, Ohlemiller KK, Shah GN, Ulmasov B, Becker TA, Waheed A, Hennig AK, Lukasiewicz PD, Sly WS (2007) Carbonic anhydrase XIV deficiency produces a functional defect in the retinal light response. Proc Natl Acad Sci USA 104:8514–8519

Oien KA, McGregor F, Butler S, Ferrier RK, Downie I, Bryce S, Burns S, Keith WN (2004) Gastrokine 1 is abundantly and specifically expressed in superficial gastric epithelium, down-regulated in gastric carcinoma, and shows high evolutionary conservation. J Pathol 203:789–797

Pan P, Leppilampi M, Pastorekova S, Pastorek J, Waheed A, Sly WS, Parkkila S (2006) Carbonic anhydrase gene expression in CA II-deficient (Car2−/−) and CA IX-deficient (Car9−/−) mice. J Physiol 571:319–327

Pan PW, Rodriguez A, Parkkila S (2007) A systematic quantification of carbonic anhydrase transcripts in the mouse digestive system. BMC Mol Biol 8:22

Parkkila S, Kaunisto K, Rajaniemi L, Kumpulainen T, Jokinen K, Rajaniemi H (1990) Immunohistochemical localization of carbonic anhydrase isoenzymes VI, II, and I in human parotid and submandibular glands. J Histochem Cytochem 38:941–947

Parkkila S, Parkkila AK, Vierjoki T, Stahlberg T, Rajaniemi H (1993) Competitive time-resolved immunofluorometric assay for quantifying carbonic anhydrase VI in saliva. Clin Chem 39:2154–2157

Parkkila S, Parkkila AK, Juvonen T, Rajaniemi H (1994) Distribution of the carbonic anhydrase isoenzymes I, II, and VI in the human alimentary tract. Gut 35:646–650

Parkkila S, Parkkila AK, Lehtola J, Reinila A, Sodervik HJ, Rannisto M, Rajaniemi H (1997) Salivary carbonic anhydrase protects gastroesophageal mucosa from acid injury. Dig Dis Sci 42:1013–1019

Pastorekova S, Parkkila S, Pastorek J, Supuran CT (2004) Carbonic anhydrases: current state of the art, therapeutic applications and future prospects. J Enzyme Inhib Med Chem 19:199–229

Rempel LA, Austin KJ, Ritchie KJ, Yan M, Shen M, Zhang DE, Henkes LE, Hansen TR (2007) Ubp43 gene expression is required for normal Isg15 expression and fetal development. Reprod Biol Endocrinol 5:13

Rodriguez A, Luukkaala T, Fleming RE, Britton RS, Bacon BR, Parkkila S (2009) Global transcriptional response to Hfe deficiency and dietary iron overload in mouse liver and duodenum. PLoS One 4:e7212

Sambrook J, Fritsch EF, Maniatis T (1989) Molecular cloning: a laboratory manual. Cold Spring Harbor Laboratory Press, New York

Schubert ML (2008) Gastric secretion. Curr Opin Gastroenterol 24:659–664

Shah GN, Ulmasov B, Waheed A, Becker T, Makani S, Svichar N, Chesler M, Sly WS (2005) Carbonic anhydrase IV and XIV knockout mice: roles of the respective carbonic anhydrases in buffering the extracellular space in brain. Proc Natl Acad Sci USA 102:16771–16776

Sly WS, Hu PY (1995) Human carbonic anhydrases and carbonic anhydrase deficiencies. Annu Rev Biochem 64:375–401

Sok J, Wang XZ, Batchvarova N, Kuroda M, Harding H, Ron D (1999) CHOP-Dependent stress-inducible expression of a novel form of carbonic anhydrase VI. Mol Cell Biol 19:495–504

Stumpo DJ, Byrd NA, Phillips RS, Ghosh S, Maronpot RR, Castranio T, Meyers EN, Mishina Y, Blackshear PJ (2004) Chorioallantoic fusion defects and embryonic lethality resulting from disruption of Zfp36L1, a gene encoding a CCCH tandem zinc finger protein of the Tristetraprolin family. Mol Cell Biol 24:6445–6455

Tumer Z, Croucher PJ, Jensen LR, Hampe J, Hansen C, Kalscheuer V, Ropers HH, Tommerup N, Schreiber S (2002) Genomic structure, chromosome mapping and expression analysis of the human AVIL gene, and its exclusion as a candidate for locus for inflammatory bowel disease at 12q13–14 (IBD2). Gene 288:179–185

Zhu Y, Paszty C, Turetsky T, Tsai S, Kuypers FA, Lee G, Cooper P, Gallagher PG, Stevens ME, Rubin E, Mohandas N, Mentzer WC (1999) Stomatocytosis is absent in "stomatin"-deficient murine red blood cells. Blood 93:2404–2410